2026, 66(6): 2898-2910
CSTR: 32112.14.j.AMS.20250950
DOI: 10.13343/j.cnki.wsxb.20250950

微生物学报
Acta Microbiologica Sinica
http://journals.im.ac.cn/actamicrocn

Research Article 研究报告

红树林紫泥弧菌 ZWAL4003 多元素代谢耦合过程实验解析

李晨[1]，王健鑫[1]，夏梓钦[1]，曾润颖[2]，曲武[1*]

1 浙江海洋大学 海洋科学与技术学院，浙江 舟山
2 自然资源部海洋生物资源开发技术创新中心，福建 厦门

李晨, 王健鑫, 夏梓钦, 曾润颖, 曲武. 红树林紫泥弧菌 ZWAL4003 多元素代谢耦合过程实验解析[J]. 微生物学报, 2026, 66(6): 2898-2910.
LI Chen, WANG Jianxin, XIA Ziqin, ZENG Runying, QU Wu. Experimental elucidation of multi-element metabolism coupling in the mangrove-derived *Vibrio ziniensis* ZWAL4003[J]. Acta Microbiologica Sinica, 2026, 66(6): 2898-2910.

摘　要：【目的】弧菌是驱动红树林沉积物中碳、氮、硫整体循环过程的重要参与者，但能够执行多种元素代谢过程的可培养弧菌菌株鲜有报道。本研究旨在验证红树林紫泥弧菌(*Vibrio ziniensis*) ZWAL4003 参与碳、氮、硫等多元素代谢的功能，并揭示相关元素循环过程的互作关系及耦合机制。【方法】综合运用基因组分析、系统进化分析、16S rRNA 基因丰度分析以及生理生化指标测定等方法探究 ZWAL4003 中潜在的元素代谢耦合过程。【结果】菌株 ZWAL4003 基因组中存在完整的三羧酸循环、氧化磷酸化、异化硝酸盐还原为铵及同化性硫还原相关基因。生理实验表明，葡萄糖、蔗糖、淀粉和甘油等碳源代谢可显著提升 ZWAL4003 的硝酸盐还原活性；而以 $NaNO_3$ 作为氮源会抑制其硫酸盐还原活性，$Na_2S_2O_3$、Na_2SO_4 和 Na_2SO_3 等硫源对硝酸盐还原活性存在抑制作用。此外，该菌株的 16S rRNA 基因近缘物种在我国东南沿海典型红树林沉积物中均有分布，相对丰度为 0.004 19%−0.073 04%，且呈现出自北向南递增的趋势。【结论】本研究证实，在 ZWAL4003 菌株中碳源利用对硝酸盐和硫酸盐还原具有促进作用，而氮源和硫源的代谢活性存在相互抑制作用，进而形成了碳-氮-硫元素代谢的耦合过程。*V. ziniensis* 在我国红树林生态系统中广泛分布，预示着该类群可能是该生态系统中元素循环耦合的重要执行者，本研究结果深化了对红树林生态系统微生物驱动的地球化学过程整体性的认知。

关键词：基因组学；红树林；弧菌；元素循环；耦合过程

资助项目：国家自然科学基金(42573055, 42303064)；自然资源部海洋生物资源开发利用工程技术创新中心开放基金(TICMBR202406)
This work was supported by the National Natural Science Foundation of China (42573055, 42303064) and the Fund of the Technology Innovation Center for Exploitation of Marine Biological Resources, MNR (TICMBR202406).
*Corresponding author. E-mail: quwu2165@zjou.edu.cn
Received: 2025-12-19; Accepted: 2026-03-11; Published online: 2026-04-07

Experimental elucidation of multi-element metabolism coupling in the mangrove-derived *Vibrio ziniensis* ZWAL4003

LI Chen[1], WANG Jianxin[1], XIA Ziqin[1], ZENG Runying[2], QU Wu[1*]

1 Marine Science and Technology College, Zhejiang Ocean University, Zhoushan, Zhejiang, China

2 Technology Innovation Center for Exploitation of Marine Biological Resources, Ministry of Natural Resources, Xiamen, Fujian, China

Abstract: [Objective] Although the coupling of carbon (C), nitrogen (N), and sulfur (S) cycles is crucial in mangrove ecosystems, direct experimental evidence from pure microbial cultures demonstrating this coupling remains scarce. This work aims to elucidate the coupling process of C, N, and S cycles in mangrove-derived *Vibrio ziniensis* ZWAL4003. **[Methods]** An integrated approach combining genomic analysis, phylogenetic analysis, 16S rRNA gene abundance quantification, and physiological-biochemical characterization was employed to explore the potential coupling process of element metabolism in ZWAL4003. **[Results]** The genome of ZWAL4003 carried genes associated with complete metabolic pathways including tricarboxylic acid cycle, oxidative phosphorylation, dissimilatory nitrate reduction to ammonium, and assimilatory sulfur reduction. Glucose, sucrose, starch, and glycerol as C sources significantly enhanced the nitrate reduction activity of ZWAL4003. $NaNO_3$ as the N source inhibited the sulfate reduction activity of ZWAL4003. $Na_2S_2O_3$, Na_2SO_4, and Na_2SO_3 as the S sources inhibited the nitrate reduction activity. Furthermore, *V. ziniensis* strains were widely distributed in the mangrove sediments along the southeast coast of China, with the relative abundance of 0.004 19%−0.073 04%, showing an increasing trend from north to south. **[Conclusion]** This study demonstrates that C source utilization promotes nitrate and sulfate reductions, while mutual inhibition exists between nitrate and sulfate reductions, forming the coupling process of C, N, and S metabolisms in ZWAL4003. The wide distribution of *V. ziniensis* strains in the mangrove ecosystems of China suggests the potential important role of *V. ziniensis* as an executor in coupling element cycles. These findings enrich our understanding of the integrity of microbe-driven geochemical processes in mangrove ecosystems.

Keywords: genomics; mangrove; *Vibrio*; element cycling; coupling process

Mangroves are rich in microbial resources that drive key processes in the chemical cycling of elements[1]. The element cycle has proved to be a comprehensive process instead of an independent one in mangroves[2]. About 30 chemical elements essential to life are coupled, thus the behavior of one element could be used to predict and manage that of other elements (e.g. carbon storage). However, the evidence of microbial pure culture that supports the multiple biogeochemical cycles and their coupling in mangrove sediments are unclear, which limits our knowledge of the ecological functions of this ecosystem.

The genus *Vibrio* represents a prevalent and ecologically significant group of microorganisms widely distributed in mangrove sediments[3-4],

water body[5], and organisms[6]. Owing to their rapid growth rates and high abundances, *Vibrio* actively participates in the cycling of C, N, and S, contributing substantially to the decomposition and turnover of organic matter[7-8]. In our previous work, strain ZWAL4003 was isolated from mangrove sediments and identified as the type strain of a novel species, *Vibrio ziniensis*[4]. Preliminary characterization revealed its involvement in complex biogeochemical processes, such as nitrate reduction and polysaccharide degradation[4], suggesting that ZWAL4003 is an ideal model organism for investigating the coupling of multiple element metabolisms driven by *Vibrio* species.

We hypothesized that in *V. ziniensis* ZWAL4003: (1) The availability of labile carbon sources would stimulate both dissimilatory nitrate reduction and assimilatory sulfate reduction activities; (2) The presence of nitrate and sulfate/sulfite would mutually inhibit the reduction of the other, suggesting potential competition for intracellular reducing equivalents. We seek to provide a theoretical foundation for understanding the interactions and material cycling processes in mangrove sediments, ultimately contributing to the informed management and conservation of this ecosystem.

1 Materials and methods

1.1 Genomic analysis of *V. ziniensis* ZWAL4003

The extraction of bacterial genomic DNA was carried out using the bacterial DNA Kit (Omega Bio-tek, USA), and the extraction operation was carried out according to the instructions. The genome was sequenced by using PacBio platform (Pacific Biosciences, USA) and was corrected by using the reads from Illumina HiSeq platform (Illumina, USA), which was completed by Shanghai Majorbio Bio-pharm Technology Co., Ltd. (China). The software of Unicycler v0.5.0 (https://github.com/rrwick/Unicycler) and SOAPdenovo2 (https://sourceforge.net/projects/soapdenovo2/) was used for genomic assembly, and Pilon v1.24 (https://github.com/broadinstitute/pilon/releases/tag/v1.24) was used for sequence correction. The coding sequences (CDSs) were predicted using Prodigal v2.6.3 (https://github.com/hyattpd/Prodigal). The metabolic pathway annotation was performed by using BLAST+ v2.3.0 (ftp://ftp.ncbi.nlm.nih.gov/blast/executables/blast+/2.3.0/) against KEGG database (http://www.genome.jp/kegg/). The sequences of tRNA and rRNA were predicted by using tRNAscan-SE v2.0 (http://trna.ucsc.edu/software/) and Barrnap v0.8 (https://github.com/tseemann/barrnap/), respectively. The analysis of gene islands, prophages, and CRISPR-Cas was completed by IslandPath-DIMOB v1.0.0 (http://www.pathogenomics.sfu.ca/islandviewer/), PHAST v1.0 (http://phast.wishartlab.com), and CRISPR Recognition Tool v1.0 (CRT, http://www.room220.com/crt), respectively. The genome plot was drawn by using Circos v0.69 (https://circos.ca/software/). The phylogenetic tree was constructed by using MEGA v6.0 (https://www.megasoftware.net/) with the neighbor-joining method and a bootstrap value of 1 000.

1.2 The determination of cell growth curve

V. ziniensis ZWAL4003 was inoculated into 50 mL 2216E medium containing 5 g/L peptone and 1 g/L yeast extract, then was cultured at 28 ℃ until OD_{600} value reached 0.8 measured by using a microplate reader (Multiskan SkyHigh, ThermoFisher Scientific Inc., USA) at a wavelength of 600 nm. Subsequently, the culture was transferred into 50 mL fresh 2216E medium containing a mass fraction of 1% additional N (peptone, yeast extract, NH_4Cl, and $NaNO_3$) and S ($Na_2S_2O_3$, Na_2SO_4, and Na_2SO_3) sources. The volume fraction of inoculation was 1%. Mixture was cultured with a rotation speed of 200 r/min at 28 ℃ for 12 h. The broth sample was taken every

2 h, and the absorbance at 600 nm of the sample was determined to characterize the growth of bacterial strain. All experiments were performed with three biological replicates.

1.3 The determination of nitrate concentration

The bacterial cells were pre-cultured according to the method in section 1.2. The broth was transferred into 50 mL 2216E medium containing $NaNO_3$ with a mass fraction of 1%. Moreover, additional C (glucose, sucrose, starch, glycerol, CMC-Na, and citrate-Na) and S ($Na_2S_2O_3$, Na_2SO_4, and Na_2SO_3) sources at a final mass fraction of 1% were respectively supplemented in this medium. Then, the medium was cultured with a rotation speed of 200 r/min at 28 ℃ until OD_{600} reached 0.8. The supernatant was sampled from the culture after centrifugation at 10 000 r/min, then NO_3^- content in supernatant was conducted by using the zinc-cadmium reduction method. Briefly, 25 mL sample was mixed with 0.5 mL $CdCl_2$ solution (20 g/L) and Zn sheets (99.99% purity), and then the mixture was shaken at 150 r/min for 10 minutes to reduce NO_3^- to NO_2^-. The absorbance at 543 nm was measured to calculate the concentration of NO_3^- based on the standard curve with a R^2 value of 0.999 4.

1.4 The measurement of sulfate concentration

The bacterial cells were pre-cultured according to the method in section 1.2. The broth was transferred into 50 mL 2216E medium containing Na_2SO_4 with a mass fraction of 1%. Moreover, additional C (glucose, sucrose, starch, glycerol, CMC-Na, and citrate-Na) and N (peptone, yeast extract, NH_4Cl, and $NaNO_3$) sources at a final mass fraction of 1% were respectively supplemented in this medium. Then, the medium was cultured with a rotation speed of 200 r/min at 28 ℃ until OD_{600} reached 0.8. The supernatant was filtered through a 0.22 μm filter and SO_4^{2-} concentration was analyzed by using an ion chromatograph (ICS-2100, Multiskan SkyHigh, ThermoFisher Scientific Inc., USA) with the eluent of 8 mmol/L Na_2CO_3/1 mmol/L $NaHCO_3$ and a flow rate of 1.0 mL/min.

1.5 The calculation of 16S rRNA gene abundances of *V. ziniensis* strains from mangrove sediments in China

The mangroves along the southeast coast of China, including Fujian, Guangdong, and Guangxi Provinces, were selected. The clean sequencing data of 16S rRNA gene of the bacterial community in these mangrove sediments were downloaded from NODE (https://www. biosino. org/node/home) under the accession numbers of OEP001343, OEP001474, OEP001673, OEP001828, OEP001935 to OEP001948, and OEP002010. for calculating the relative abundance of *V. ziniensis* strains. The sequences with a similarity ≥97% to the 16S rRNA gene of ZWAL4003 were selected as the target sequences, and the relative abundance of *V. ziniensis* strain was calculated as the percentage of target sequence number to the total sequence number in the dataset.

1.6 Experimental design and statistical analysis

Three biological replicates were set for all biochemical assays in current study. Significant difference analysis was performed by using Student's *t*-test in R software (version 4.5.2; https://www.r-project.org/).

2 Results and analysis

2.1 Metabolic gene analysis of carbon, nitrogen, and sulfur sources in ZWAL4003 genomics

The complete genome of ZWAL4003 included two complete chromosomes with the lengths of 1 443 184 bp (G+C content 42.13%) and 3 207 372 bp (G+C content 43.12%), respectively (Figure 1). A total of 86.16% of sequences in ZWAL4003 genome was protein-coding, and 10, 10, and 11 genes in the genome encoded 16S, 23S,

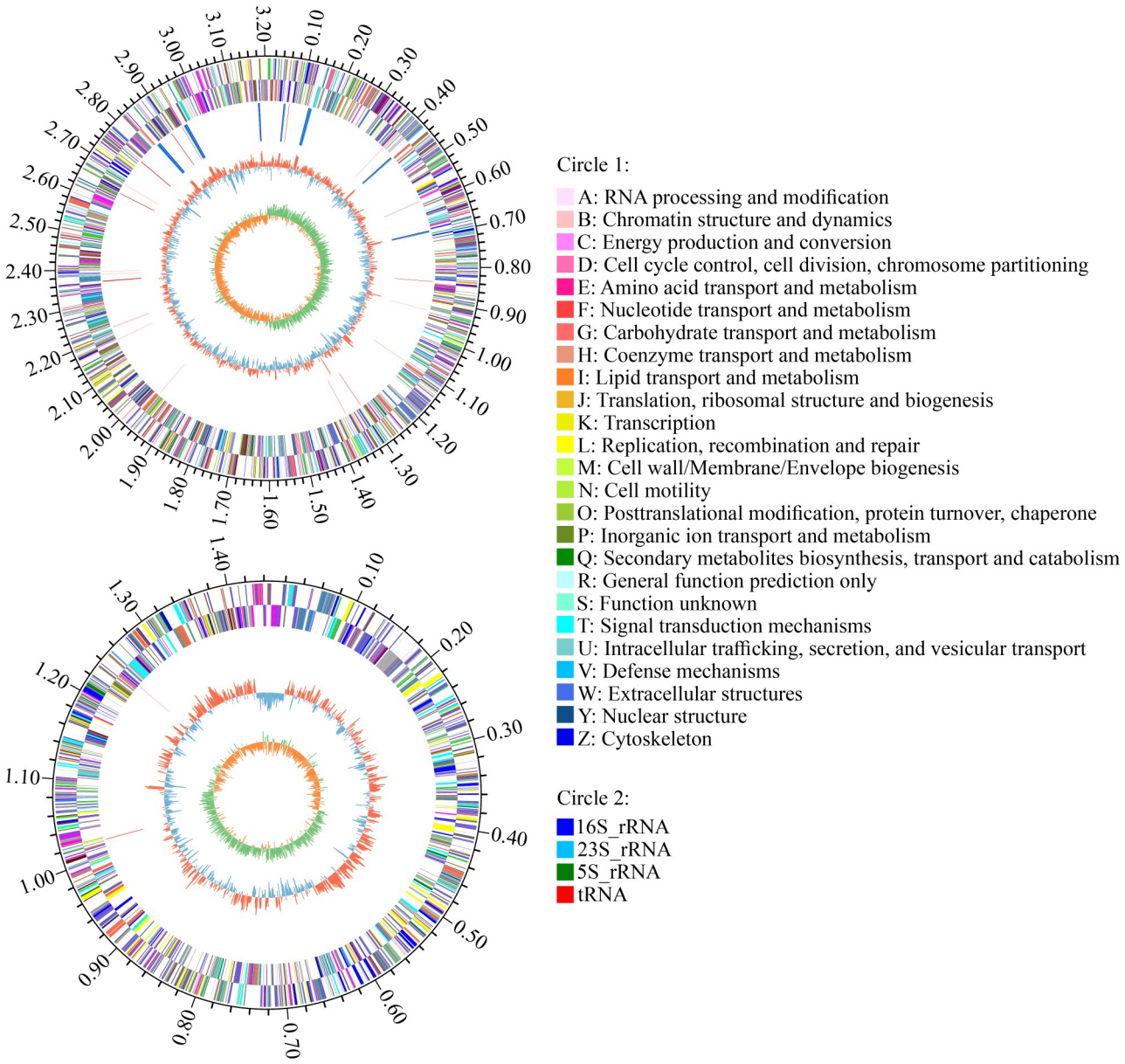

Figure 1 The genome map of two chromosomes in *Vibrio ziniensis* ZWAL4003. The outermost circle is the marker of genome size. The second and third cycles are protein-coding sequences on positive and negative chains, and colors indicate the functional classification in COG database. The fourth circle is rRNA and tRNA genes. The fifth circle is the G+C content. The outward red color indicates that the G+C content in this region is higher than the average G+C content. The inward blue color indicates that the G+C content in this region is lower than the average G+C content. The innermost circle is the G+C skew value.

and 5S rRNA, respectively. Ten gene islands, 2 prophages, and 2 CRISPRs were annotated in ZWAL4003 genome. The key genes involved in C cycle, such as sugar metabolisms, tricarboxylic acid (TCA) cycle, and oxidative phosphorylation, were found in the genome sequences.

Furthermore, the complete pathways that participated in dissimilatory nitrate reduction to

ammonium (DNRA; including 1 *napA*, 1 *napB*, 2 *nirB*, and 2 *nirD* genes) and assimilatory sulfur reduction (ASR; including 2 *cysC*, 2 *cysD*, 2 *cysN*, 1 *cysH*, 1 *cysI*, and *cysJ*) were annotated. These genes were phylogenetically closest to those with the accession numbers of WP 171138587.1 (Figure 2A), WP 416922594.1 (Figure 2B), WP 167410564.1 (Figure 2C), WP 171138556.1 (Figure 2D), WP 102941627.1 (Figure 2E), WP 171138557.1 (Figure 2F), WP 416921474.1 (Figure 2G), WP 202649566.1 (Figure 2H), WP 102966295.1 (Figure 2I), WP 275659734.1 (Figure 2J), WP 416923142.1 (Figure 2K), WP 416923140.1 (Figure 2L), WP 416921476.1 (Figure 2M), WP407834869.1 (Figure 2N), and WP 175579797.1 (Figure 2O) from *Vibrio* species.

2.2 The influences of carbon and sulfur sources on nitrate metabolism of *V. ziniensis* ZWAL4003

Glucose, sucrose, starch, and glycerol significantly increased the nitrate removal rate by 29.9%, 31.3%, 30.3%, and 14.6%, respectively (P<0.05). However, CMC-Na and citrate-Na decreased the nitrate removal rate by 47.9% and 88.3%, respectively (Figure 3A; P<0.05). The addition of sulfur sources of $Na_2S_2O_3$, Na_2SO_4, and Na_2SO_3 significantly decreased the nitrate removal rate of *V. ziniensis* ZWAL4003, especially $Na_2S_2O_3$ and Na_2SO_3 completely inhibited the nitrate removal activity of this strain (Figure 3B; P<0.05). Therefore, glucose, sucrose, starch, and glycerol enhanced nitrate reduction activity of *V. ziniensis* ZWAL4003, whereas CMC-Na, citrate-Na, $Na_2S_2O_3$, Na_2SO_4, and Na_2SO_3 were inhibitory for this activity.

2.3 The influences of carbon and nitrogen sources on sulfate metabolism of *V. ziniensis* ZWAL4003

Glucose, sucrose, starch, and glycerol significantly increased the sulfate removal rate by 51.2%, 37.6%, 55.9%, and 27.0%, respectively (P<0.05). CMC-Na and citrate-Na significantly decreased the sulfate removal rate by 73.6% and 48.7%, respectively (Figure 3C; P<0.05). The nitrogen sources of peptone and NH_4Cl had no obvious influence on sulfate removal rate, while $NaNO_3$ significantly decreased the sulfate removal rate by 92.9% (Figure 3D; P<0.05). Therefore, peptone and NH_4Cl did not change the sulfate reduction activity of *V. ziniensis* ZWAL4003. Furthermore, glucose, sucrose, starch, and glycerol could improve the sulfate reduction activity of *V. ziniensis* ZWAL4003, while this activity was inhibited by CMC-Na, citrate-Na, and $NaNO_3$.

2.4 The influences of nitrogen and sulfur sources on cell growth of *V. ziniensis* ZWAL4003

Compared to the control group, the peptone promoted the cell growth of *V. ziniensis* ZWAL4003, whereas the yeast extract, NH_4Cl, and $NaNO_3$ delayed the growth of *V. ziniensis* ZWAL4003. Notably, the cell accumulation of *V. ziniensis* ZWAL4003 was lowest with the nitrogen source of $NaNO_3$ (Figure 3E). The additional sulfur sources of $Na_2S_2O_3$, Na_2SO_4, and Na_2SO_3 slowed down the cell growth of *V. ziniensis* ZWAL4003, and Na_2SO_3 mostly delayed the growth of *V. ziniensis* ZWAL4003 among these sulfur sources followed by $Na_2S_2O_3$ (Figure 3F).

2.5 The putative coupling process of carbon, nitrogen, and sulfur metabolisms in *V. ziniensis* ZWAL4003

Based on the above results, we inferred the interplay among the cell growth, nitrate and sulfate reductions as follows: (i) Most substrates for carbon utilization and oxidative phosphorylation enhanced the activities of nitrate and sulfate reductions; (ii) The substrates of nitrate and sulfate reductions exerted reciprocal inhibitory effects; (iii) The substrates of nitrate and sulfate reductions delayed cell growth. Based on biochemical data, the coupling process of carbon-nitrogen-sulfur metabolisms in *V. ziniensis* ZWAL4003 was supposed in Figure 4.

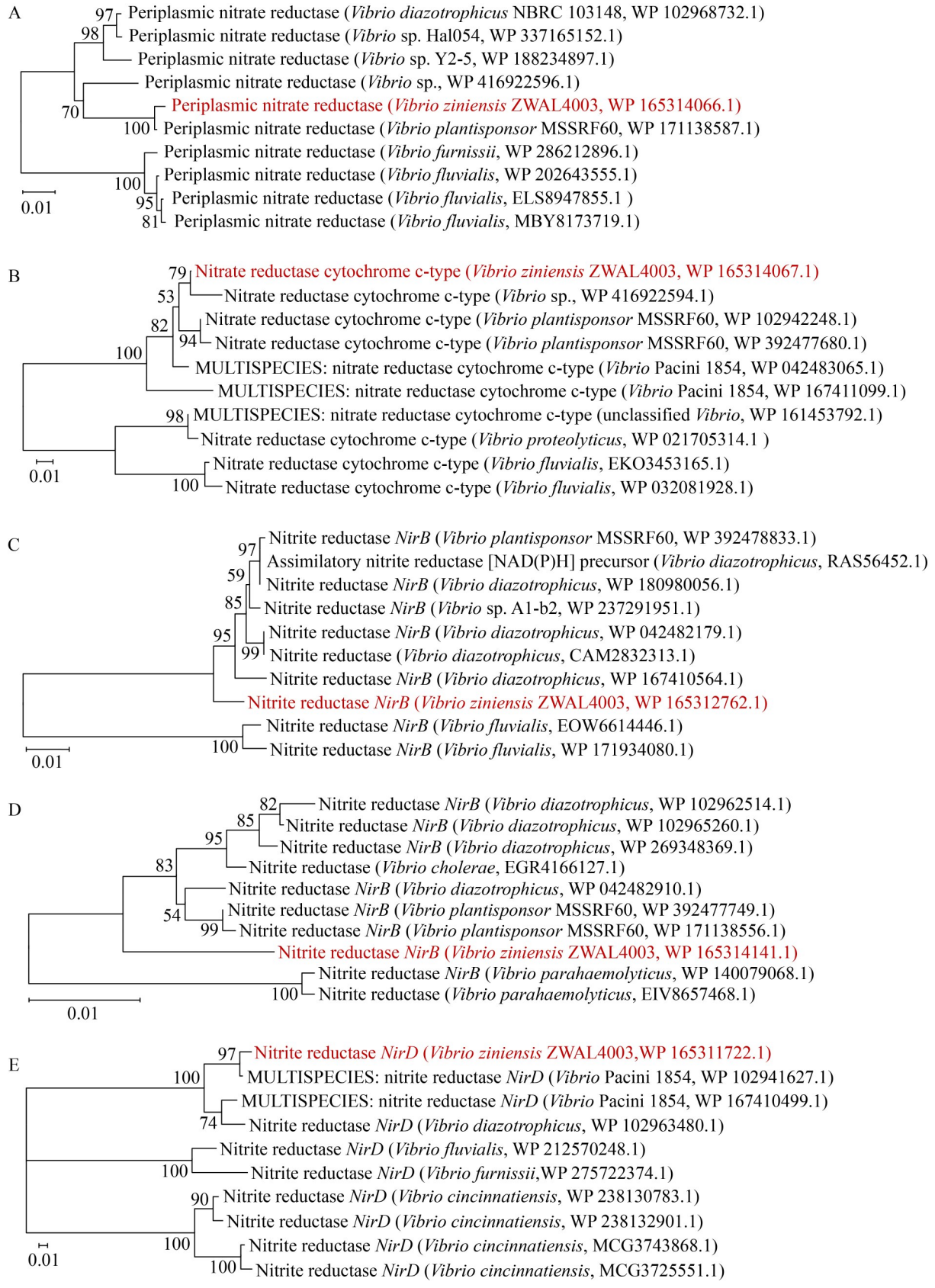
A
97 Periplasmic nitrate reductase (*Vibrio diazotrophicus* NBRC 103148, WP 102968732.1)
98 Periplasmic nitrate reductase (*Vibrio* sp. Hal054, WP 337165152.1)
Periplasmic nitrate reductase (*Vibrio* sp. Y2-5, WP 188234897.1)
Periplasmic nitrate reductase (*Vibrio* sp., WP 416922596.1)
70 Periplasmic nitrate reductase (*Vibrio ziniensis* ZWAL4003, WP 165314066.1)
100 Periplasmic nitrate reductase (*Vibrio plantisponsor* MSSRF60, WP 171138587.1)
Periplasmic nitrate reductase (*Vibrio furnissii*, WP 286212896.1)
100 Periplasmic nitrate reductase (*Vibrio fluvialis*, WP 202643555.1)
95 Periplasmic nitrate reductase (*Vibrio fluvialis*, ELS8947855.1)
81 Periplasmic nitrate reductase (*Vibrio fluvialis*, MBY8173719.1)
0.01
B
79 Nitrate reductase cytochrome c-type (*Vibrio ziniensis* ZWAL4003, WP 165314067.1)
53 Nitrate reductase cytochrome c-type (*Vibrio* sp., WP 416922594.1)
82 Nitrate reductase cytochrome c-type (*Vibrio plantisponsor* MSSRF60, WP 102942248.1)
94 Nitrate reductase cytochrome c-type (*Vibrio plantisponsor* MSSRF60, WP 392477680.1)
100 MULTISPECIES: nitrate reductase cytochrome c-type (*Vibrio* Pacini 1854, WP 042483065.1)
MULTISPECIES: nitrate reductase cytochrome c-type (*Vibrio* Pacini 1854, WP 167411099.1)
98 MULTISPECIES: nitrate reductase cytochrome c-type (unclassified *Vibrio*, WP 161453792.1)
Nitrate reductase cytochrome c-type (*Vibrio proteolyticus*, WP 021705314.1)
0.01
Nitrate reductase cytochrome c-type (*Vibrio fluvialis*, EKO3453165.1)
100 Nitrate reductase cytochrome c-type (*Vibrio fluvialis*, WP 032081928.1)
C
97 Nitrite reductase *NirB* (*Vibrio plantisponsor* MSSRF60, WP 392478833.1)
Assimilatory nitrite reductase [NAD(P)H] precursor (*Vibrio diazotrophicus*, RAS56452.1)
59 Nitrite reductase *NirB* (*Vibrio diazotrophicus*, WP 180980056.1)
85 Nitrite reductase *NirB* (*Vibrio* sp. A1-b2, WP 237291951.1)
95 Nitrite reductase *NirB* (*Vibrio diazotrophicus*, WP 042482179.1)
99 Nitrite reductase (*Vibrio diazotrophicus*, CAM2832313.1)
Nitrite reductase *NirB* (*Vibrio diazotrophicus*, WP 167410564.1)
Nitrite reductase *NirB* (*Vibrio ziniensis* ZWAL4003, WP 165312762.1)
Nitrite reductase *NirB* (*Vibrio fluvialis*, EOW6614446.1)
100 Nitrite reductase *NirB* (*Vibrio fluvialis*, WP 171934080.1)
0.01
D
82 Nitrite reductase *NirB* (*Vibrio diazotrophicus*, WP 102962514.1)
85 Nitrite reductase *NirB* (*Vibrio diazotrophicus*, WP 102965260.1)
95 Nitrite reductase *NirB* (*Vibrio diazotrophicus*, WP 269348369.1)
83 Nitrite reductase (*Vibrio cholerae*, EGR4166127.1)
Nitrite reductase *NirB* (*Vibrio diazotrophicus*, WP 042482910.1)
54 Nitrite reductase *NirB* (*Vibrio plantisponsor* MSSRF60, WP 392477749.1)
99 Nitrite reductase *NirB* (*Vibrio plantisponsor* MSSRF60, WP 171138556.1)
Nitrite reductase *NirB* (*Vibrio ziniensis* ZWAL4003, WP 165314141.1)
Nitrite reductase *NirB* (*Vibrio parahaemolyticus*, WP 140079068.1)
100 Nitrite reductase (*Vibrio parahaemolyticus*, EIV8657468.1)
0.01
E
97 Nitrite reductase *NirD* (*Vibrio ziniensis* ZWAL4003,WP 165311722.1)
100 MULTISPECIES: nitrite reductase *NirD* (*Vibrio* Pacini 1854, WP 102941627.1)
MULTISPECIES: nitrite reductase *NirD* (*Vibrio* Pacini 1854, WP 167410499.1)
74 Nitrite reductase *NirD* (*Vibrio diazotrophicus*, WP 102963480.1)
Nitrite reductase *NirD* (*Vibrio fluvialis*, WP 212570248.1)
100 Nitrite reductase *NirD* (*Vibrio furnissii*,WP 275722374.1)
90 Nitrite reductase *NirD* (*Vibrio cincinnatiensis*, WP 238130783.1)
Nitrite reductase *NirD* (*Vibrio cincinnatiensis*, WP 238132901.1)
100 Nitrite reductase *NirD* (*Vibrio cincinnatiensis*, MCG3743868.1)
0.01
100 Nitrite reductase *NirD* (*Vibrio cincinnatiensis*, MCG3725551.1)

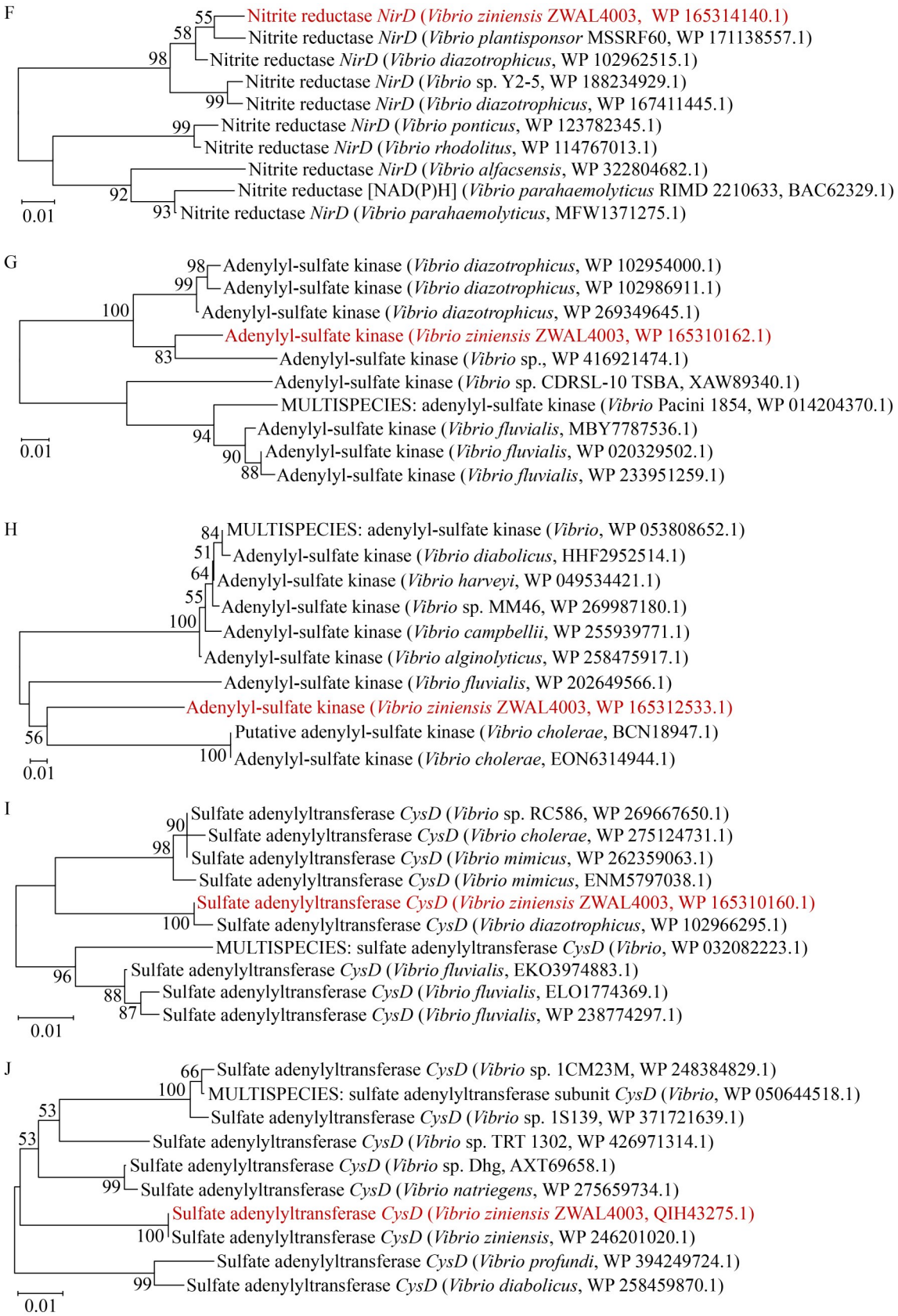
F
Nitrite reductase NirD (Vibrio ziniensis ZWAL4003, WP 165314140.1)
Nitrite reductase NirD (Vibrio plantisponsor MSSRF60, WP 171138557.1)
Nitrite reductase NirD (Vibrio diazotrophicus, WP 102962515.1)
Nitrite reductase NirD (Vibrio sp. Y2-5, WP 188234929.1)
Nitrite reductase NirD (Vibrio diazotrophicus, WP 167411445.1)
Nitrite reductase NirD (Vibrio ponticus, WP 123782345.1)
Nitrite reductase NirD (Vibrio rhodolitus, WP 114767013.1)
Nitrite reductase NirD (Vibrio alfacsensis, WP 322804682.1)
Nitrite reductase [NAD(P)H] (Vibrio parahaemolyticus RIMD 2210633, BAC62329.1)
Nitrite reductase NirD (Vibrio parahaemolyticus, MFW1371275.1)
0.01
G
Adenylyl-sulfate kinase (Vibrio diazotrophicus, WP 102954000.1)
Adenylyl-sulfate kinase (Vibrio diazotrophicus, WP 102986911.1)
Adenylyl-sulfate kinase (Vibrio diazotrophicus, WP 269349645.1)
Adenylyl-sulfate kinase (Vibrio ziniensis ZWAL4003, WP 165310162.1)
Adenylyl-sulfate kinase (Vibrio sp., WP 416921474.1)
Adenylyl-sulfate kinase (Vibrio sp. CDRSL-10 TSBA, XAW89340.1)
MULTISPECIES: adenylyl-sulfate kinase (Vibrio Pacini 1854, WP 014204370.1)
Adenylyl-sulfate kinase (Vibrio fluvialis, MBY7787536.1)
Adenylyl-sulfate kinase (Vibrio fluvialis, WP 020329502.1)
Adenylyl-sulfate kinase (Vibrio fluvialis, WP 233951259.1)
0.01
H
MULTISPECIES: adenylyl-sulfate kinase (Vibrio, WP 053808652.1)
Adenylyl-sulfate kinase (Vibrio diabolicus, HHF2952514.1)
Adenylyl-sulfate kinase (Vibrio harveyi, WP 049534421.1)
Adenylyl-sulfate kinase (Vibrio sp. MM46, WP 269987180.1)
Adenylyl-sulfate kinase (Vibrio campbellii, WP 255939771.1)
Adenylyl-sulfate kinase (Vibrio alginolyticus, WP 258475917.1)
Adenylyl-sulfate kinase (Vibrio fluvialis, WP 202649566.1)
Adenylyl-sulfate kinase (Vibrio ziniensis ZWAL4003, WP 165312533.1)
Putative adenylyl-sulfate kinase (Vibrio cholerae, BCN18947.1)
Adenylyl-sulfate kinase (Vibrio cholerae, EON6314944.1)
0.01
I
Sulfate adenylyltransferase CysD (Vibrio sp. RC586, WP 269667650.1)
Sulfate adenylyltransferase CysD (Vibrio cholerae, WP 275124731.1)
Sulfate adenylyltransferase CysD (Vibrio mimicus, WP 262359063.1)
Sulfate adenylyltransferase CysD (Vibrio mimicus, ENM5797038.1)
Sulfate adenylyltransferase CysD (Vibrio ziniensis ZWAL4003, WP 165310160.1)
Sulfate adenylyltransferase CysD (Vibrio diazotrophicus, WP 102966295.1)
MULTISPECIES: sulfate adenylyltransferase CysD (Vibrio, WP 032082223.1)
Sulfate adenylyltransferase CysD (Vibrio fluvialis, EKO3974883.1)
Sulfate adenylyltransferase CysD (Vibrio fluvialis, ELO1774369.1)
Sulfate adenylyltransferase CysD (Vibrio fluvialis, WP 238774297.1)
0.01
J
Sulfate adenylyltransferase CysD (Vibrio sp. 1CM23M, WP 248384829.1)
MULTISPECIES: sulfate adenylyltransferase subunit CysD (Vibrio, WP 050644518.1)
Sulfate adenylyltransferase CysD (Vibrio sp. 1S139, WP 371721639.1)
Sulfate adenylyltransferase CysD (Vibrio sp. TRT 1302, WP 426971314.1)
Sulfate adenylyltransferase CysD (Vibrio sp. Dhg, AXT69658.1)
Sulfate adenylyltransferase CysD (Vibrio natriegens, WP 275659734.1)
Sulfate adenylyltransferase CysD (Vibrio ziniensis ZWAL4003, QIH43275.1)
Sulfate adenylyltransferase CysD (Vibrio ziniensis, WP 246201020.1)
Sulfate adenylyltransferase CysD (Vibrio profundi, WP 394249724.1)
Sulfate adenylyltransferase CysD (Vibrio diabolicus, WP 258459870.1)
0.01

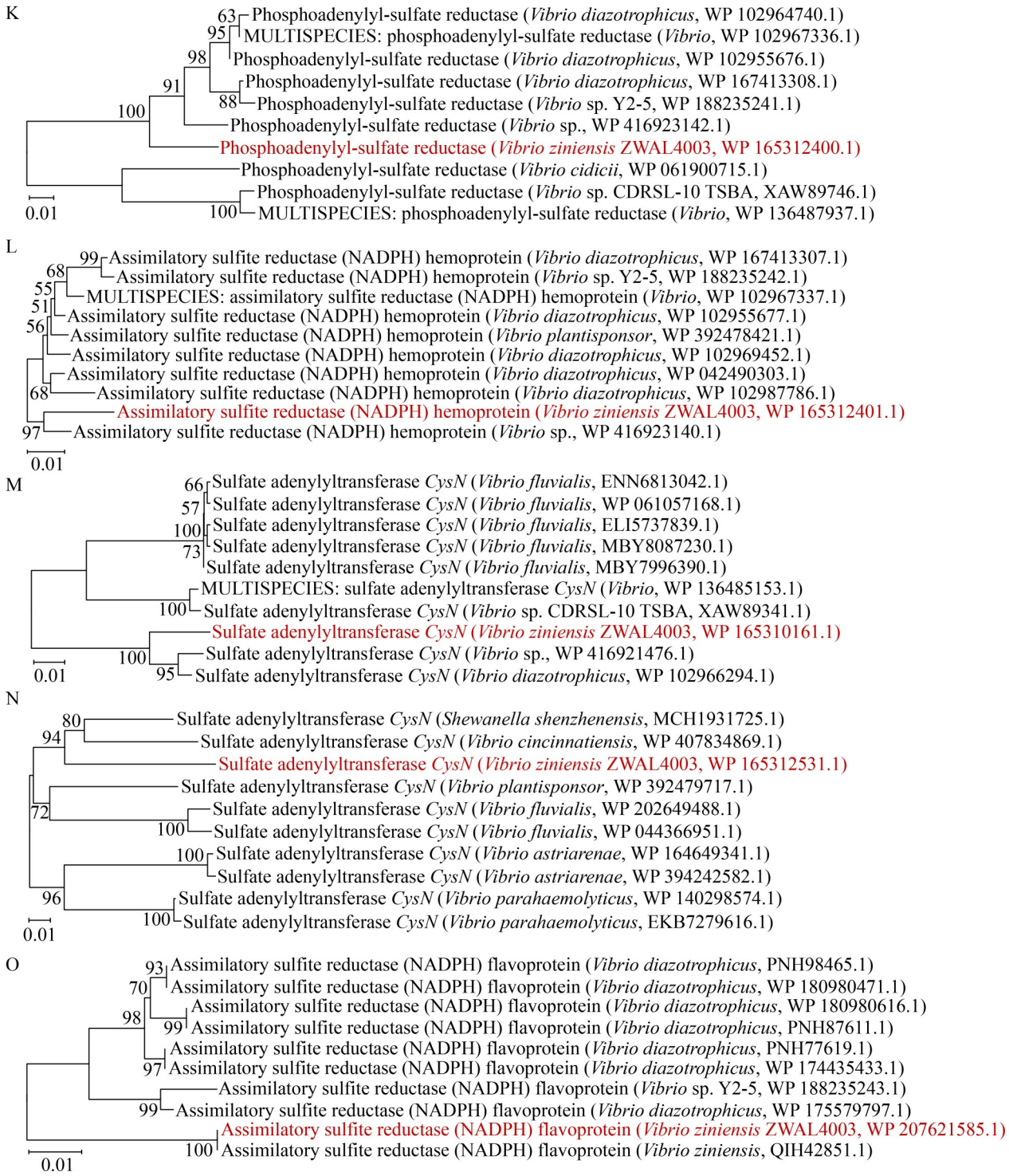

Figure 2 Phylogenetic analysis of dissimilatory nitrate reduction to ammonium (DNRA) and assimilatory sulfur reduction (ASR) genes by using the neighbor-joining method. A: *napA* gene; B: *napB* gene; C and D: *nirB* genes; E and F: *nirD* genes; G and H: *cysC* genes; I and J: *cysD* genes; K: *cysH* gene; L: *cysI* gene; M and N: *cysN* genes; O: *cysJ* gene.

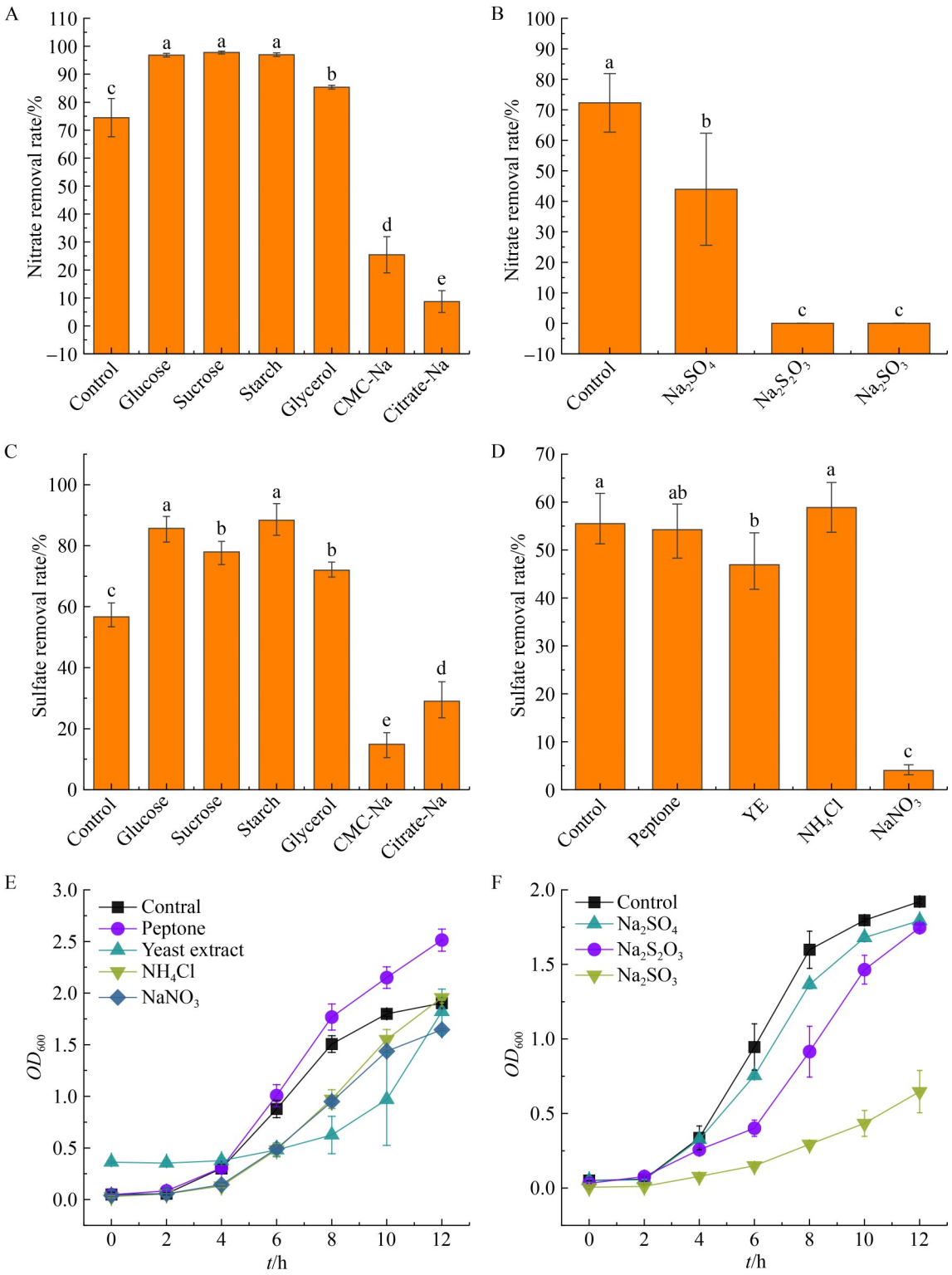

Figure 3 Effects of carbon, nitrogen, and sulfur sources on the bioactivities of ZWAL4003. The effects of carbon (A) and sulfur (B) sources on nitrate removal rate; The effects of carbon (C) and nitrogen (D) sources on sulfate removal rate; The effects of nitrogen (E) and sulfur (F) sources on cell growth.

2.6 The distribution of *V. ziniensis* strains in mangrove sediments along the coast of China

Four locations with mangrove forests along the southeast coast of China, including Fujian, Guangdong, and Guangxi Provinces, were selected for calculating the relative abundance of 16S rRNA gene of *V. ziniensis* strains. The relative abundances of *V. ziniensis* strains were respectively 0.004 19%, 0.006 25%, 0.031 85%, and 0.073 04% in the mangrove sediments from these locations, and roughly increased from north to south in China (Figure 5).

3 Discussion

Although the coupling of carbon, nitrogen, and sulfur cycles has been proposed in mangrove ecosystems based on metagenomic data, direct evidence from pure cultures that experimentally demonstrates such coupling remains limited[9]. Previous studies have identified potential functional guilds—such as sulfur-driven denitrifiers or methane oxidizers coupled with sulfate reducers—through metagenome-assembled genomes (MAGs)[2], but these findings rely on sequence assembly and inference, which may introduce uncertainties[10]. In contrast, the present study provided experimental evidence from a pure

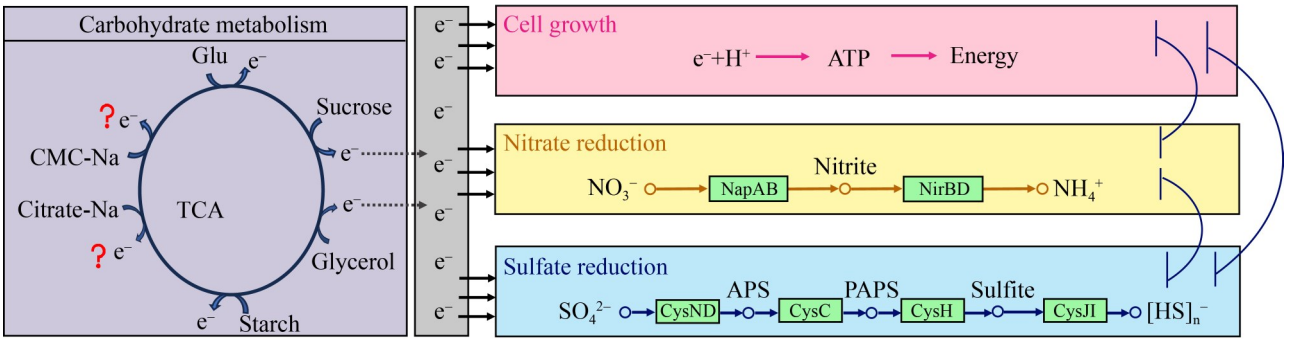

Figure 4 The putative process and mechanism of carbon-nitrogen-sulfur metabolism coupling in ZWAL4003.

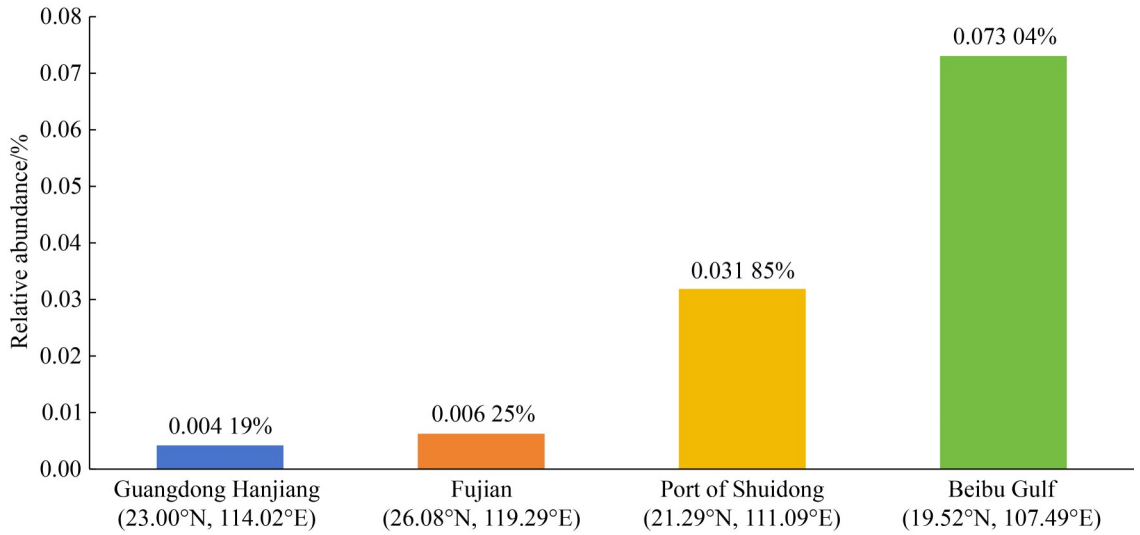

Figure 5 The relative abundance of *Vibrio ziniensis* strain in the mangrove sediments from Fujian, Guangdong, and Guangxi provinces in China.

culture of *V. ziniensis* ZWAL4003 to elucidate the coupling mechanisms among carbon, nitrogen, and sulfur metabolisms. By integrating genomic analysis with physiological assays, we offered an experimental basis for understanding multi-element metabolic coupling at the strain level.

This work demonstrated the existence of the coupling of carbon, nitrogen, and sulfur metabolisms in pure culture through biochemical experiments. This evidence avoids using the complex and error-prone algorithm for pathway analysis in metagenomic data. The results showed an actual promoting effect of carbon utilization on nitrate and sulfate reductions and a competition relationship between nitrate and sulfate reductions in *V. ziniensis* ZWAL4003, thereby providing a solid supporter for the biogeochemical cycle coupling in mangrove sediments. As a fast-growth genus[8], *Vibrio* species greatly contributed to the material cycles in marine environments[7], including mangrove sediments[11]. Based on the biochemical measurement results, we suppose that the abundant storage of carbon sources and sulfate in mangrove sediments causes the strong positive coupling of carbon utilization and sulfate reduction and saves the limited nitrate in the sediments for potentially supporting the primary productivity of this ecosystem[12] due to the competition between nitrate and sulfate reductions in *V. ziniensis* ZWAL4003.

The 16S rRNA gene of ZWAL4003, the type strain in *V. ziniensis*[4], is phylogenetically clustered with those of *V. plantisponsor* MSSRF60 and *V. diazotrophicus* ATCC 33466, and these two strains possess the abilities of nitrogen fixation and nitrate reduction[13-14], which suggests that this cluster positively involved in the nitrogen loss and supplement in sediments and soils. Furthermore, our findings revealed a wide distribution of *V. ziniensis* strains in the mangrove sediments along the southeast coast of China, indicating that the strains belonging to this species might be the potential important center that connected carbon, nitrogen, and sulfur cycles to form a holistic rather than an isolated element cycle system in mangroves from China. Nevertheless, we still need the relevant activities of the strain in the field environment in future research to determine its true ecological function in mangrove.

The coupling of carbon (C), nitrogen (N), and sulfur (S) cycles is likely driven by electron transfer derived from microbial oxidation of organic matter[15-17]. Accordingly, we propose a putative coupling mechanism in *V. ziniensis* ZWAL4003: electrons generated from the oxidation of readily utilizable carbon sources (e.g., glucose) could be channeled to support the reductive steps of both dissimilatory nitrate reduction and assimilatory sulfate reduction, thereby enhancing these processes[18-19], thereby enhancing the reduction activities. Conversely, the observed mutual inhibition between nitrate and sulfate reduction may stem from competition for intracellular reducing equivalents (electrons). Interestingly, CMC-Na and citrate-Na unexpectedly decreased the reduction activities for both nitrate and sulfate. We speculate that these specific carbon sources might redirect cellular reducing power towards alternative metabolic pathways, altering electron flow. These results point to complex, strain-specific metabolic networks and electron partitioning, underscoring the need for future studies employing metabolic flux and electron transfer analyses in *V. ziniensis* ZWAL4003.

4 Conclusion

This study elucidates the genetic potential and physiological mechanism for the coupling of multiple element metabolisms in *V. ziniensis* ZWAL4003. Genomic analysis revealed complete pathways for oxidative phosphorylation, DNRA, and ASR. Physiological experiments provided compelling evidence that carbon source utilization promotes both nitrate and sulfate reductions, while a competitive interaction, likely for reducing equivalents, leads to mutual inhibition between the two pathways. The wide distribution of *V. ziniensis* strains in mangrove sediments along China's coast

suggests that this coupling mechanism is ecologically relevant, positioning this species as a potential player in multiple elemental cycles within this important ecosystem. This work provided evidence from a pure culture, widening our understanding of holistic, microbe-driven geochemical process in mangroves.

Credit authorship contribution statement

LI Chen: Experiment implementation, data curation, visualization, and draft writing; WANG Jianxin: Formal analysis, project administration; XIA Ziqin: Methodology, sample collection; ZENG Runying: Technical support, bacterial strain supply; QU Wu: Project supervision, draft revision, funding acquisition. All authors commented on previous versions of the manuscript, read and approved the final manuscript.

Declaration of Competing Interest

The authors declare no competing financial interest.

References

[1] Zhang YX, Xia ZQ, Zuo YQ, Ding JJ, Wang JX, Qu W. The increase of particle size shifts the biogeochemical cycle functions of mineral-associated microorganisms and weakens the mineral-associated organic carbon sink in mangrove soils[J]. Applied and Environmental Microbiology, 2024, 90(10): e01272-24.

[2] Qian L, Yu XL, Gu H, Liu F, Fan YJ, Wang C, He Q, Tian Y, Peng YS, Shu LF, Wang SQ, Huang ZJ, Yan QY, He JG, Liu GL, Tu QC, He ZL. Vertically stratified methane, nitrogen and sulphur cycling and coupling mechanisms in mangrove sediment microbiomes[J]. Microbiome, 2023, 11: 71.

[3] Gao ZM, Xiao J, Wang XN, Ruan LW, Chen XL, Zhang YZ. *Vibrio xiamenensis* sp. nov., a cellulase-producing bacterium isolated from mangrove soil[J]. International Journal of Systematic and Evolutionary Microbiology, 2012, 62(Pt_8): 1958-1962.

[4] Wu J, Qu W, Lai QL, Pei SX, Zhang TY, Zhuang Y, Chan ZH, Zeng RY. *Vibrio ziniensis* sp. nov., isolated from mangrove sediments[J]. International Journal of Systematic and Evolutionary Microbiology, 2021, 71(4): 004777.

[5] Ibangha II, Digwo DC, Ozochi CA, Enebe MC, Ateba CN, Chigor VN. A meta-analysis on the distribution of pathogenic *Vibrio* species in water sources and wastewater in Africa[J]. Science of the Total Environment, 2023, 881: 163332.

[6] Xu JQ, Yang S, Yang LR. *Vibrio natriegens* as a host for rapid biotechnology[J]. Trends in Biotechnology, 2022, 40(4): 381-384.

[7] Thompson JR, Polz MF. Dynamics of *Vibrio* populations and their role in environmental nutrient cycling[M]//The Biology of Vibrios. Washington, DC, USA: ASM Press, 2014: 190-203.

[8] Sampaio A, Silva V, Poeta P, Aonofriesei F. *Vibrio* spp. life strategies, ecology, and risks in a changing environment[J]. Diversity, 2022, 14(2): 97.

[9] Dong HL, Zeng Q, Sheng YZ, Chen CM, Yu GH, Kappler A. Coupled iron cycling and organic matter transformation across redox interfaces[J]. Nature Reviews Earth & Environment, 2023, 4(9): 659-673.

[10] Lynn HM, Gordon JI. Sequential co-assembly reduces computational resources and errors in metagenome-assembled genomes[J]. Cell Reports Methods, 2025, 5(3): 101005.

[11] Panda SK, Das S. Potential of plant growth-promoting microbes for improving plant and soil health for biotic and abiotic stress management in mangrove vegetation[J]. Reviews in Environmental Science and Bio, 2024, 23(3): 801-837.

[12] Naidoo G. Dwarfing in mangroves: a review[J]. Physiologia Plantarum, 2025, 177(4): e70411.

[13] Rameshkumar N, Gomez-Gil B, Spröer C, Lang E, Dinesh Kumar N, Krishnamurthi S, Nair S, Roque A. *Vibrio plantisponsor* sp. nov., a diazotrophic bacterium isolated from a mangrove associated wild rice (*Porteresia coarctata* Tateoka)[J]. Systematic and Applied Microbiology, 2011, 34(7): 487-493.

[14] Guerinot ML, West PA, Lee JV, Colwell RR. *Vibrio diazotrophicus* sp. nov., a marine nitrogen-fixing bacterium[J]. International Journal of Systematic Bacteriology, 1982, 32(3): 350-357.

[15] Jiang YG, Shi MM, Shi L. Molecular underpinnings for microbial extracellular electron transfer during biogeochemical cycling of earth elements[J]. Science China Life Sciences, 2019, 62(10): 1275-1286.

[16] Wen WR, Liu TC, Fan SQ, Tan X, Lu Y, Xing DF, Liu BF, Ren NQ, Xie GJ. Dissimilatory nitrate reduction to ammonium driven by different electron donors: mechanisms, recent advances, and future perspectives[J]. Chemical Engineering Journal, 2025, 507: 160625.

[17] Zhang Y, Liu T, Li MM, Hua ZS, Evans P, Qu YN, Tan S, Zheng M, Lu H, Jiao JY, Lücker S, Daims H, Li WJ, Guo JH. Hot spring distribution and survival mechanisms of thermophilic comammox *Nitrospira*[J]. The ISME Journal, 2023, 17(7): 993-1003.

[18] Pandey CB, Kumar U, Kaviraj M, Minick KJ, Mishra AK, Singh JS. DNRA: a short-circuit in biological N-cycling to conserve nitrogen in terrestrial ecosystems[J]. Science of the Total Environment, 2020, 738: 139710.

[19] Saito K. Sulfur assimilatory metabolism. the long and smelling road[J]. Plant Physiology, 2004, 136(1): 2443-2450.